Environmental Science & Technology

ARTICLE

pubs.acs.org/est

Schwertmannite Formation Adjacent to Bacterial Cells in a Mine Water Treatment Plant and in Pure Cultures of *Ferrovum myxofaciens*

Sabrina Hedrich,[*,†,⊥] Heinrich Lünsdorf,[‡] Reinhard Kleeberg,[§] Gerhard Heide,[§] Jana Seifert,[†,¶] and Michael Schlömann[†]

[†]Interdisciplinary Ecological Center, TU Bergakademie Freiberg, Leipziger Strasse 29, 09599 Freiberg, Germany

[‡]Department of Vaccinology and Applied Microbiology, Helmholtz Centre for Infection Research, Inhoffenstrasse 7, D-38124 Braunschweig

[§]Institute of Mineralogy, TU Bergakademie Freiberg, Brennhausgasse 14, 09599 Freiberg, Germany

Supporting Information

ABSTRACT: Schwertmannite has previously been found in iron- and sulfate-rich mine waters at pH 2.8−4.5. In the present study, schwertmannite ($Fe_8O_8(OH)_6SO_4$) was shown to be the major mineral in a mine water treatment plant at pH 3, in which ferrous iron is mainly oxidized by bacteria belonging to the species *Ferrovum myxofaciens*. Strain EHS6, which is closely related to the type strain of *Fv. myxofaciens*, was isolated from the pilot plant and characterized as an acidophilic, iron-oxidizing bacterium. In contrast to the pilot plant, the mineral phase formed by a pure culture of *Fv. myxofaciens* EHS6 was a mixture of schwertmannite and jarosite ($KFe_3(SO_4)_2(OH)_6$). In contrast to other reports of neutrophilic, iron-oxidizing bacteria, acidophilic microorganisms in the pilot plant and cultures of strain EHS6 did not show encrustation of the cell surface or deposition of minerals inside the cell, though a few cells appeared to be in contact with jarosite crystals. It was concluded that no direct biomineralization occurred in the pilot plant or in laboratory cultures. The lack of encrustation of bacterial cells in the pilot plant is considered advantageous since the cells are still able to get in contact with ferrous iron and the iron oxidation process in the mine water treatment plant can proceed.

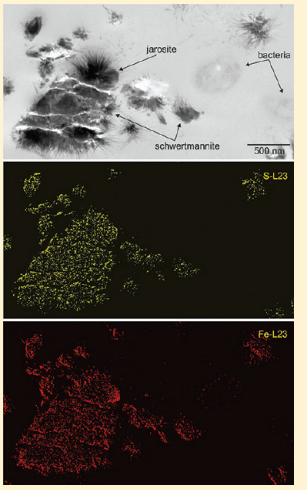

INTRODUCTION

Acid mine drainage (AMD) is a widespread environmental problem caused by deep or surface mining of metal ores or lignite. Waters resulting from oxidative dissolution of exposed minerals are characterized by low pH and high loads of sulfate, iron, and other toxic down metals, thus causing environmental pollution.

Mine waters represent a favored habitat for various acidophilic bacteria, which can use ferrous iron or reduced inorganic sulfur compounds (RISC) as electron donors under aerobic conditions. The chemical oxidation of ferrous iron at acidic pH is decelerated, and thus, iron oxidation at low pH is largely catalyzed by iron-oxidizing bacteria, which use oxygen as electron acceptor.[1] At circumneutral pH, in contrast, ferrous iron is highly unstable toward molecular oxygen, and for this reason, microbial iron oxidation by neutrophilic microorganisms is more prevalent in anoxic or microaerobic zones.[2]

Ferric iron ions, resulting from microbial iron-oxidation activities, are crucial not only for dissolution of minerals such as pyrite but also for iron mineral formation. The composition and structure of such mineral dependents on the respective environmental conditions, e.g., pH, redox potential, and sulfate content of the waters. Besides the physicochemical parameters, various interactions between bacteria and minerals have been reported. Some neutrophilic bacteria protect themselves against mineral encrustation, as is the case with *Gallionella ferruginea* which selectively deposit iron hydroxy minerals on their stalks.[3,4] Bacteria in biofilms are known to cover themselves with exopolymeric material in conjunction with iron minerals.[5] Electron microscopy studies of environmental samples, dominated by neutrophilic bacteria, showed cell walls and cell products of the bacteria encrusted with ferrihydrite.[6,7] In contrast, experiments with several cultures of neutrophilic, anaerobic, Fe(II)-oxidizing bacteria showed that some of the strains, which were tested, were not encrusted with the minerals formed in the cultures.[8,9]

The mineral initially formed in sulfate-rich AMD at pH 2.8−4.5 is schwertmannite, a poorly ordered oxyhydroxysulfate with the idealized formula $Fe_8O_8(OH)_6SO_4$.[10] It can differ in color, morphology and elemental composition depending on the pH value and other hydrogeochemical conditions. Schwertmannite is metastable with respect to goethite at circumneutral pH, resulting in a release of sulfate. At low pH, in the presence of

Received: July 27, 2010
Accepted: August 12, 2011
Revised: July 31, 2011
Published: August 12, 2011

Table 1. Chemical Parameters of Pilot Plant Water during the Sampling Period[a]

Sample	Sampling time	pH	T [°C]	E_h [mV]	Fe(II) [mg/l]	Fe(III) [mg/l]	SO_4^{2-} [mg/l]
S14_06	July 2006	3.2	19.8	736	167	168	2100
SM_06	August 2006	3.1	21.4	736	202	135	2160
SC_06							
SI_06							
S23_07	Jan.- Aug. 2007	2.8 - 3.1	16.5	737	121	160	1440
SH_09	September 2009	3.5	14.5	767	166	66	1551

[a] Samples SM_06, SC_06, and SI_06 were taken at the same time from different locations in the pilot plant to show homogeneity of minerals in the system.

different monovalent cations (e.g., K^+, Na^+, NH_4^+), and at high sulfate concentrations, schwertmannite transforms to jarosite. Schwertmannite has been detected globally in several environments at different pH values.[11−13]

The interactions of acidophilic bacteria with iron minerals in AMD environments are so far only poorly understood. Electron microscopic studies on the bacterial−mineral interface of sediment samples from Rio Tinto[14] have shown iron minerals directly associated with exopolymeric substances (EPS), the cell wall, the periplasm, and the cytoplasmic membrane. Similar results were obtained by Fortin et al. showing the cell wall of *Acidithiobacillus ferrooxidans* encrusted with jarosite-like minerals.[15] Benzerara and co-workers observed mineralized vesicles in samples from iron- and arsenic-rich mine water from Carnoulès mine (France). They concluded that those vesicles could have been present in former studies of extensively mineralized samples but had been overlooked.[16] Moreover, in bioleaching experiments of chalcopyrite with *At. ferrooxidans*, biofilm formation in association with the encrustation of the EPS by jarosite was observed.[17] In contrast, Eneroth and co-workers concluded from low protein contents in mineral samples that the cell walls of *At. ferrooxidans* had no influence on the precipitation process of schwertmannite or jarosite.[18]

The bacterial community investigated in this study is involved in the oxidation of iron in a mine water treatment plant, used for the purification of iron- and sulfur-rich mine waters in Lusatia.[19] Previous investigations of the bacterial community showed the dominance of a so far not formally described species of *Betaproteobacteria Ferrovum myxofaciens*, which was tentatively named *Ferribacter polymyxa* in former publications,[20] but has been renamed recently.

The aim of the present work was to demonstrate that the mineral phase formed in the pilot plant and in laboratory cultures is, in fact, schwertmannite, suitable for use as a pigment and chemical adsorbent.[21] Electron microscopy was used to investigate the possible bacterial impact on mineral formation by electron energy-loss spectroscopic and microdiffraction analysis.

EXPERIMENTAL SECTION

Plant Mineral Samples. The principle of biological mine water treatment was carried out in a pilot plant located in the area of the opencast pit Nochten, Lusatia (Saxony), as described by Heinzel et al.[22] The pilot plant was operated under stable conditions with only slight changes in chemical parameters as presented in Table 1. During the process, iron hydroxy sulfate precipitates covered the carrier materials, the wall, and bottom of the plant.

Minerals were collected and air-dried from various positions in the pilot plant during a period from July 2006 to September 2009. Samples were collected ad hoc at time scales ranging from single days to months. In contrast to the general sampling procedure, sample S23_7 was taken from a heterogeneous mixture of mineral samples cumulatively collected from the pilot plant over eight months and stored in the open air.

Bacterial Strain and Growth Conditions. Strain EHS6 was isolated from treatment plant waters using a modified version of solid overlay plates ("iFeo" medium).[23] The plates containing basal salts, trace elements, and 25 mM ferrous iron at pH ∼ 2.5 were spread-inoculated with 100 μL of pilot plant water and incubated at room temperature for 3 weeks (for a detailed description of the mentioned methods see Supporting Information). Single ferric-iron stained colonies were transferred onto new plates and later inoculated into liquid mineral salt medium at pH 2.5 containing 25 mM ferrous iron sulfate and incubated at room temperature.[23,24] After successful growth, indicated by a color change of the medium from colorless to red-orange, biomass was removed from the liquid cultures for DNA extraction and 16S rRNA gene sequence analysis.[24] Strain EHS6 shared 99% identical positions with *Ferrovum myxofaciens* strain P3G (nominated type strain) on 16S rDNA level and on the basis of this was identified as a member of the species. Additionally strain EHS6 was shown to be an autotrophic, acidophilic iron-oxidizer, which forms streamer growth by production of massive EPS (S.Hedrich, unpublished data). This is similar to strain PSTR of the species *Fv. myxofaciens* described by Rowe et al.[25] and the type strain P3G (D.B. Johnson, personal communication).

For further experiments, strain EHS6 was grown in 100 mL liquid cultures inoculated with 2% (v/v) of an EHS6 preculture in 250 mL Erlenmeyer baffle flasks and incubated at room temperature with shaking (130 rpm). One plastic Sessil strip, as used in the pilot plant, was added to each culture flask to enable the attachment of bacteria for biofilm formation. A sterile control flask containing mineral salt medium pH 2.5 and ferrous iron sulfate was incubated under the same conditions.

Ferrous iron oxidation was monitored using the Ferrozine colorimetric method.[26] In addition, pH measurements were carried out on the liquid phase.

Characterization of the Mineral Phase. The composition of the solid phase formed in the pilot plant and batch culture was determined by X-ray powder diffraction (XRD), X-ray fluorescence (XRF), and inductively coupled plasma optical emission spectroscopy (ICP-OES). Total organic carbon (TOC) content was determined from the solid state sample. For a detailed description of the mentioned methods, see Supporting Information.

Electron Microscopic Analyses. Mineral samples formed in the bulk phase of the Erlenmeyer baffle flasks were taken at the late exponential growth phase. Additional Sessil strips, applied to the shake flasks for biofilm formation, were removed when an initial biofilm was established, i.e., 5 days after strip exposure.

Samples were fixed immediately upon recovery in 50 mL plastic tubes with 2% (v/v) glutardialdehyde in 20 mM HEPES buffer (pH 7.5) and were stored until further use. Samples were prepared according to Lünsdorf et al.[27] for conventional transmission electron microscopy (CTEM) of thin sections and scanning electron microscopy (SEM). Further, biofilm aliquots were embedded in epoxy resin, and 40 nm ultrathin sections were analyzed by electron energy-loss spectroscopy. Energy-filtered

Table 2. Properties of Ferric Iron Precipitates[a]

			elemental composition		
				[% wt/wt]	
sample	color Munsell	XRD pattern	molar ratio of Fe/S	N	C
Pilot Plant Samples					
S14_06	6.3YR 5/8.6	Sch, J	6.4	<0.05	0.8
SM_06	7.5YR 5.5/8	Sch	6.4	<0.05	0.8
SC_06	7.5YR 5.5/8	Sch	6.1	<0.05	0.8
SI_06	7.5YR 5.5/8	Sch	6.4	<0.05	0.8
S23_07	6.3YR 4.6/8.6	Sch, G	6.6	<0.05	2.8
SH_09	7.5YR 5.5/8	Sch	n.d.	<0.05	1.5
EHS6 Culture Sample					
S6	n.d.	Sch, J	5.2	<0.05	0.7

[a] Sch: schwertmannite; J: jarosite; G: goethite.

selected area electron diffraction (SAED) was done on 50 nm ultrathin sections (detailed procedures are described in Supporting Information). Sections were cut normal to the biofilm plane, showing the intrinsic biofilm architecture from the Sessil substratum surface to the biofilm top surface. Tracing of acidic constituents within the biofilm matrix by cationic colloidal ThO_2 was performed as described by Lünsdorf et al.[28]

RESULTS

Bacterial Growth and Mineral Formation in Cultures of *Ferrovum myxofaciens* Strain EHS6. The bacterium was grown in a basal salt medium supplemented with ferrous iron to study mineral formation in the cultures. Cultures of strain EHS6 completely oxidized the soluble ferrous iron in batch experiments within five days (Figure S1, Supporting Information).

Initial mineral formation in batch cultures could be observed as an orange turbidity, when ferrous iron oxidation had started (Figure S1, Supporting Information). After ferrous iron was completely oxidized, minerals began to deposit onto the bottom and wall of the flask. The minerals precipitated in the culture medium were dark red to brown in color and turned yellow after more than four weeks of incubation. No changes in pH or ferrous iron concentration and, thus, no mineral precipitation were observed in the aseptic control flask.

Characterization of Pilot Plant and Flask Culture Ferric Iron Precipitates. Mineral samples collected from the pilot plant and the EHS6 cultures were analyzed by X-ray diffraction and for their chemical composition (Table 2).

All pilot plant samples contained schwertmannite as the dominant mineral, but it must be noticed that significant amounts of amorphous components or poorly crystalline phases (e.g., ferrihydrite) cannot be excluded on the basis of the XRD pattern (Table 2, Figure S2, Supporting Information). Sample S14_06 was the only pilot plant sample, which contained small amounts of jarosite (general formula $MFe_3(SO_4)_2(OH)_6$, M = K^+, Na^+, H_3O^+, NH_4^+), and sample S23_07 showed traces of crystalline goethite, which was confirmed by a higher Fe/S ratio. According to the general schwertmannite formula $Fe_{16}O_{16}(OH)_y(SO_4)_z$ (where $16 - y = 2z$ and $2.0 \leq z \leq 3.5$),[29] the theoretical Fe/S ratio of schwertmannite is expected to be between 4.6 and 8. As the samples were collected at different intervals over a long period (Table S1, Supporting Information) and since the pilot plant is an open system, where the composition of the inflowing water can vary, e.g., with respect to small amounts of silicon from sand or clay particles, sample composition can also be slightly variable. The color of the precipitates (Table 2), according to Munsell soil color chart, was in agreement with that expected for schwertmannite.

Furthermore, the high similarity in XRD pattern, chemical composition, and color of samples SI_06, SC_06, and SM_06, taken at the same time from different positions in the pilot plant, demonstrate the homogeneity of the pilot plant product. The solid phase formed in cultures of strain EHS6, in contrast, showed a mixture of jarosite and schwertmannite, as indicated by sharp peaks for jarosite and broad peaks for schwertmannite (Figure S2, Supporting Information). Due to the higher amount of jarosite in this sample, the Fe/S molar ratio of 5.2 was slightly lower than in pilot plant samples containing schwertmannite. The jarosite formed in the growth medium of strain EHS6 had elevated potassium content relative to the low potassium-jarosite content of the pilot plant (determined by EELS and XRF). The range of nitrogen (<0.05% wt/wt) and organic carbon (0.8−2.8% wt/wt) contents were similar in all samples investigated.

Micromorphology of Fe(III) Minerals from Pilot Plant Samples by Electron Microscopy. Transmission electron micrographs of ultrathin sections of solid samples from the pilot plant showed characteristic mineral aggregates (Figure 1a), which were composed of an inner amorphous core, surrounded by a dense coat of thin fibers. In general, these so-called hedgehog-like aggregates ranged from 350 to 700 nm in diameter, and the peripheral needles, also called whiskers, had a length of up to 260 nm and a width of ca. 10 nm. These micromorphological features have been reported and are characteristic for schwertmannite.[10,29]

Bacterial cells were found either several micrometers away from the minerals or almost inside mineral clusters, in which no encrustation of the cell surface by mineral deposits could be observed (Figure 1a). Application of colloidal, cationic thorium dioxide as tracer of negative charges, such as acidic mucopolysaccharides and/or nucleic acids, allowed detection of a dense, but only thin layer of acidic EPS surrounding the cells (Figure S3, Supporting Information, electron dense dots).

Minerals Formed in the Planktonic Phase or in Biofilms of *Fv. myxofaciens* EHS6 Cultures. Ferrous iron oxidation in cultures of strain EHS6, isolated from the pilot plant, caused ochre precipitates similar to those in pilot plant samples. Transmission electron micrographs of these samples showed the typical schwertmannite microstructure. The core of the minerals was as dense as the ones of the pilot plant minerals, but the whiskers seemed to be thinner. The length of the needles ranged up to 220 nm, and mineral aggregates had a diameter of 270 to 350 nm further arranged in oligo- and polyclusters (Figure 1b).

Occasionally, EHS6 cells formed "aggregates" of 30 to 60 cells which were embedded and individually surrounded by a dense matrix of acidic EPS, intensely stained by colloidal ThO_2 (Figure 1b). The secreted EPS material remained free from mineralization (Figure 1b).

Additionally, scanning electron micrographs of a biofilm of strain EHS6 grown on Sessil substratum revealed numerous granular minerals (Figure 2a) and a well-defined biofilm structure associated with filamentous EPS excreted by the bacteria (Figure 2b). No pronounced acidic EPS were visible in EHS6 culture biofilms

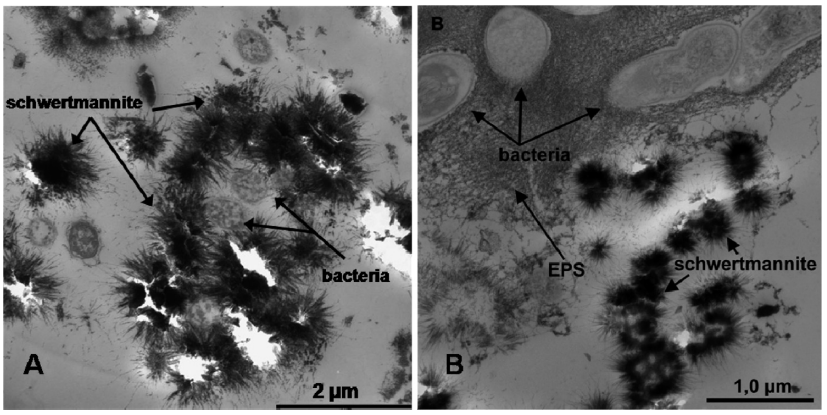

Figure 1. Transmission electron micrographs of ThO_2-stained thin sections of (A) ferric-iron minerals from the pilot plant showing characteristic schwertmannite mineral aggregates surrounding the bacteria and (B) of the *Fv. myxofaciens* strain EHS6 cultivated under acidic conditions in a basal salt medium. Samples were taken from suspension at the beginning of the stationary phase.

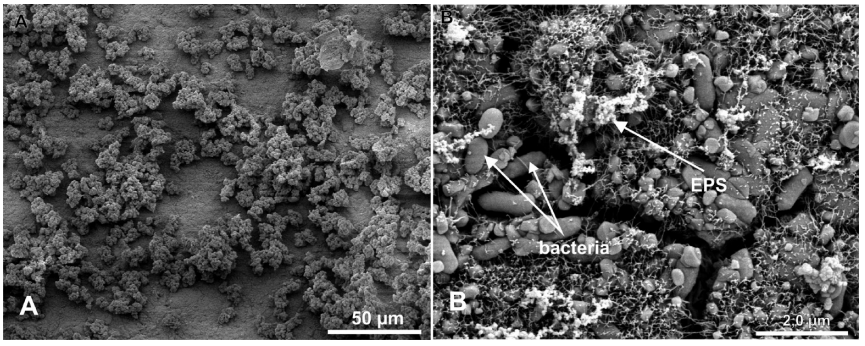

Figure 2. Scanning electron micrographs of a biofilm sample of *Fv. myxofaciens* strain EHS6 grown on Sessil in a basal salt medium containing 25 mM ferrous iron at an initial pH of 2.5 for 13 days. (A) Overview of the samples surface showing granular schwertmannite minerals. (B) Higher magnification of the biofilm indicating bacteria and EPS in the sample.

after staining with thorium dioxide. Even when staining for reductive sugar EPS-moieties, according to the silver-proteinate method of Thiéry,[30] which acts on vicinal glycols in cis configuration, no such reactive groups could be detected as EPS constituents.

The bacteria in the biofilm were found to be organized in groups of 3 to 8 cells in close vicinity to the schwertmannite mineral, while bacterial surfaces were smooth and obviously free of mineral deposits (Figure 2). Besides the hedgehog-like schwertmannite aggregates, pseudocubic jarosite crystals (240 to 500 nm in length and 120 to 290 nm in width) with a smooth surface were detected. The jarosite crystals were occasionally found to partially embed bacterial cells (Figure 3).

Micro-SAED analysis of schwertmannite aggregates and jarosite crystals was performed within a measuring aperture of 152 nm in diameter at the sample level. The corresponding electron diffractogram of poorly crystalline schwertmannite revealed a characteristic ring pattern with a *d*-spacing of the first ring of 0.254 nm. Additionally, as is indicated by white dots, arc-like diffraction revealed the partially fibrillar character of the mineral, which evidently reflects the whiskers (Figure 4a,b). Jarosite, on the other hand, showed distinct crystallinity on diffraction and a trigonal crystal system (Figure 4c,d). Thus, electron diffractometric data completely confirm X-ray diffraction studies at the microcrystallite level.

Electron Energy-Loss Spectroscopy (EELS) of Mineral Phases in the EHS6 Biofilm by Energy-Filtered Transmission Electron Microscopy (EF-TEM). EELS is a powerful method in material sciences for performing microanalyses at the nanoscale and electronic structure levels. EELS spectra are highly similar to those obtained by X-ray absorption spectroscopy.[31] Compared to energy-dispersive X-ray (EDX) microanalysis, elemental mapping by electron spectroscopic-imaging (ESI) with an EF-TEM is more sensitive and is performed within a quarter of the time at higher spatial resolution.[32]

EELS spectra of the biofilm from EHS6 cultures showed schwertmannite and jarosite to be discernible mainly by the absence or presence of potassium. Visually the two minerals were discernible by their intrinsic micromorphology. Characteristically, jarosite showed a prominent energy-loss near-edge structure (ELNES)-fingerprint of sulfate at the S-L2,3 edge (Figure 5b, red curve) and the double-peak of the K-L2,3 edge by parallel-EELS (PEELS) spot analysis. Adversely, within the limit of the 28 nm electron beam spot size, the corresponding schwertmannite matrix showed only weak signals for sulfur or rather sulfate and potassium, thus indicating their reduced concentration in this mineral (Figure 5b, blue curve). In general, high S-signal intensities as peaks in the spectrum were correlated to high elemental concentrations in the sample, as it was revealed by ESI analysis of sulfur within peripheral jarosite crystals (Figure 5e). Correspondingly, only weak sulfur intensities within the schwertmannite amorphous core were recognized.

The same schwertmannite spot showed a higher iron content of the inner core area relative to faint iron intensities in the jarosite periphery (Figure 5d). This was also evident from higher

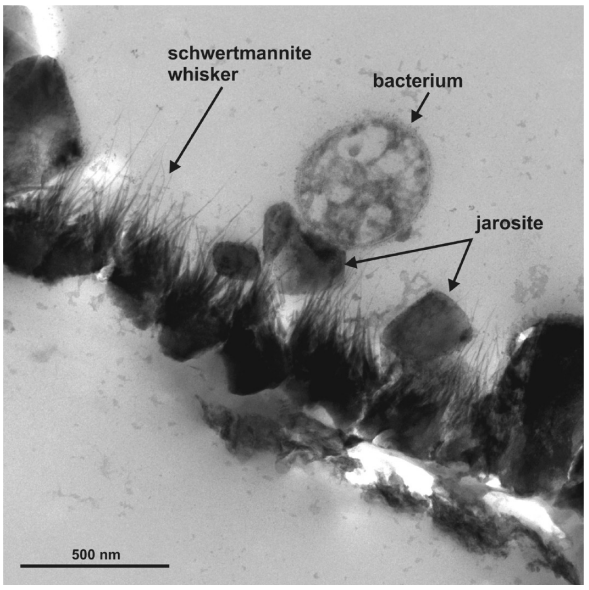

Figure 3. Transmission electron micrographs of ThO_2 stained sections of *Fv. myxofaciens* EHS6 cultivated under acidic conditions in a basal salt medium. Samples were taken at the beginning of the stationary phase. The pictures show schwertmannite and jarosite in one sample and contact of jarosite with the bacterial cell.

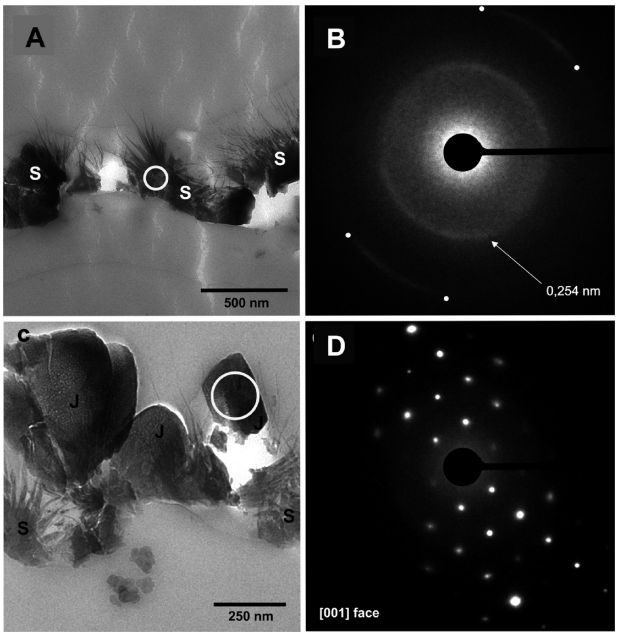

Figure 4. SAED of schwertmannite microaggregates (A, B) and jarosite crystallites (C, D) from a Sessil biofilm of *Fv. myxofaciens* EHS 6 cultures. Measuring areas (A, C) are encircled and indicative of corresponding diffractograms (B, D). S = schwertmannite; J = jarosite. White dots (B) flank an arc-like diffraction, which is indicative of a partially fibrillar appearance of the material.

peak intensities of schwertmannite-iron (but slightly lower oxygen peak intensities) relative to jarosite (with slightly higher oxygen peaks) (Figure 5c). Additionally, a chemical shift of the oxygen main peak of jarosite (538.7 eV) versus schwertmannite (539.6 eV) was observed, and correspondingly, Fe-L3 maxima of 710.9 and 711.3 eV were measured from spectra, calibrated to π^* of the C−K edge of ERL-resin at 287.5 eV for schwertmannite and jarosite.

Figures 3 and S4, Supporting Information, display the close association of jarosite to the underlying schwertmannite fiber coating and/or to the amorphous center, but the contacts appeared mainly to these nanoscale surface structures. They were rarely observed within the schwertmannite amorphous core (see S-intensities in Figure 5e), which leads to the suggestion that jarosite crystal growth is intimately associated with the schwertmannite and/or to the solute milieu. Within the analytical detection limits, mineral deposition in statu nascendi did not occur on the cell surface of EHS6 cells, which left mineralogenesis restricted to the mineral phases, but still linked to the physiological and catalytic sphere of influence of the bacterial cell (Figure S4, Supporting Information).

DISCUSSION

While mineralization patterns for some bacteria−mineral associations have been investigated in considerable detail, schwertmannite formation in this respect has received relatively little attention.[8,33,34,45] In the present study, the mineral phase formed in a mine water treatment plant and in pure cultures of a novel genus of *Betaproteobacteria* was characterized, and electron-microscopic studies were carried out to investigate possible interactions between microorganisms and mineral formation.

Mineral Formation. The main mineral formed in the pilot plant (mixed bacterial culture) at pH 3.0 was schwertmannite, which showed the typical hedgehog-like structure, while jarosite and goethite sometimes occurred in trace amounts. The mineral phase present in cultures of *Fv. myxofaciens* strain EHS6 (growth medium pH 2.6) mainly consisted of schwertmannite and jarosite.

The different composition of the mineral phase in the pilot plant (open system) and cultures of *Fv. myxofaciens* EHS6 could be a result of the slightly different geochemical conditions (e.g., pH, metal concentrations, redox potential, and temperature) between pilot plant AMD water and the synthetic growth medium used in laboratory experiments. Schwertmannite is predominantly formed in waters characterized by a pH around 3.0 and high sulfate content as well as by the occurrence of both ferrous and ferric iron.[35] It often occurs in association with jarosite, which is formed at pH < 3 and requires cations for its formation.[18] In mineral samples gained from EHS6 cultures, potassium could be identified by EELS, leading to the assumption that potassium has directed the formation of potassium jarosite. However, a direct formation of jarosite under the given chemical conditions is hindered by the kinetically favored poorly ordered schwertmannite structure.[35] However, transformation of schwertmannite to jarosite has previously been described for cultures of *Acidithiobacillus ferrooxidans* at different pH values,[33] and it can occur in solutions containing an appropriate jarosite-directing cation, for example, at pH 2.1 ± 0.05.[36] The medium used to cultivate strain EHS6 contained sodium (0.07 mM) and potassium (0.5 mM) as well as ammonium (0.9 mM) in less than millimolar concentrations. Gramp et al. reported the precipitation of K^+-jarosite starting at concentrations of 4 mM potassium in the medium and the absence of schwertmannite in samples containing ≥12 mM K^+.[37] Compared to other forms of jarosite, K^+-jarosite requires the lowest level of monovalent cations in solution for its formation.[37] Concerning all these facts, it can be assumed that schwertmannite transformed into K^+-jarosite according to the formula 1, while the pH of the

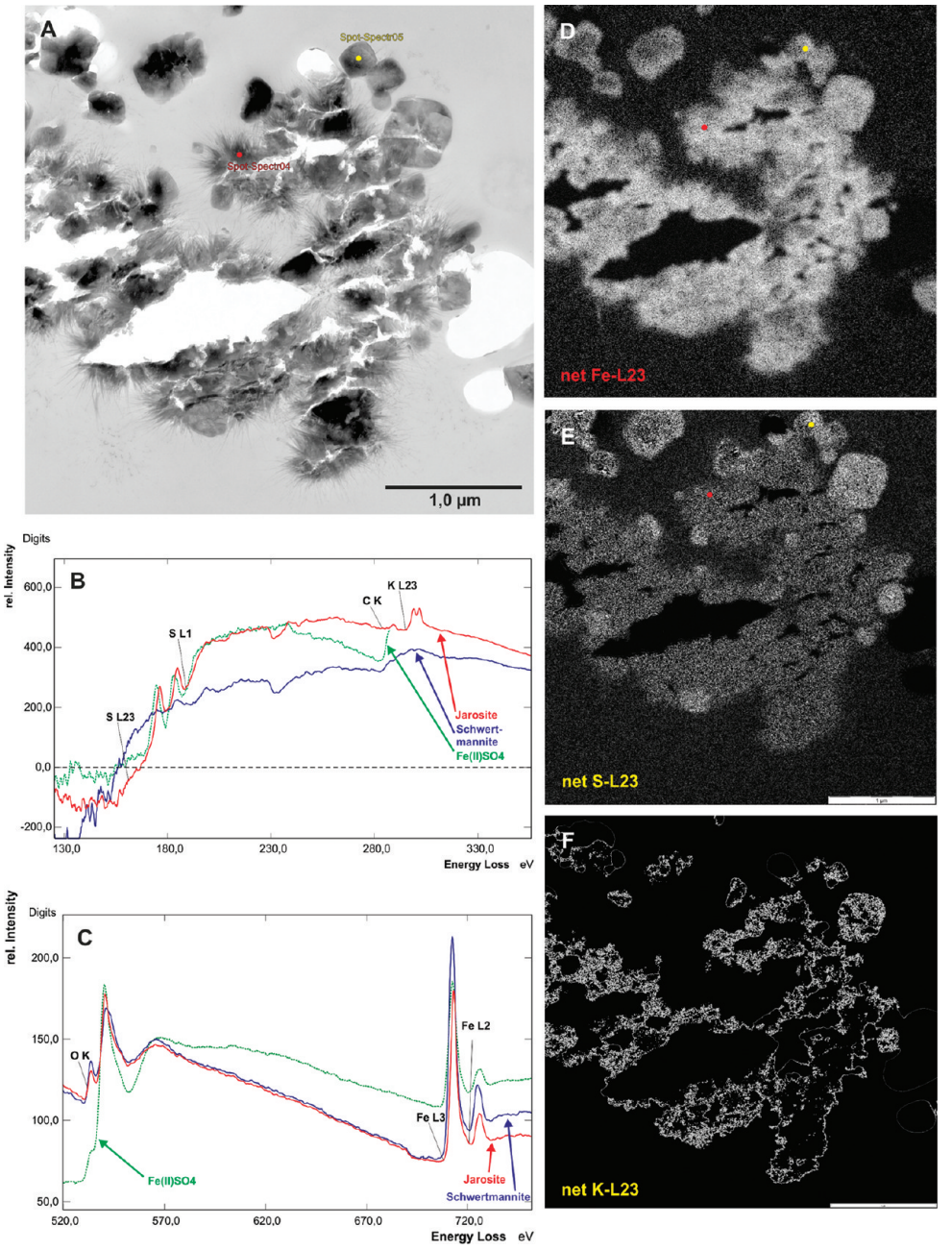

Figure 5. EELS analysis of coensembled schwertmannite and jarosite minerals within biofilms of strain EHS6. (A) "In situ" view of a mixed-mineral conglomerate with marked positions of WR-spotPEELS acquisitions by 25 nm spotsize (a, d, e); WR-spotPEELS spectra of schwermannite (dark blue) and jarosite (red) are shown in (B) and (C). Iron (D) and sulfur (E) concentrations are shown for jarosite crystals relative to schwertmannite core clusters. Spot-PEELS and reference spectrum as indicated. (F) Adequate K-L2,3 elemental map; because of C−K tailing holes in the section are smoothly outlined, not indicating the presence of potassium.

medium increased.[38]

$$3Fe_8O_8(SO_4)(OH)_6 + 6H_2O + 8K^+ + 13SO_4^{2-} + 18H^+ \rightarrow 8KFe_3(SO_4)_2(OH)_6 \quad (1)$$

Jarosite, compared to schwertmannite, contains more sulfate, resulting in the lower Fe/S molar ratio of 1.5. This fact was reflected by ICP-OES measurements showing the ratio in the S6 sample (from cultures of strain EHS6) to be 5.2 (Table 2).

EELS data of schwertmannite dense core regions showed low sulfate content, relative to jarosite. The sulfate content in schwertmannite minerals can vary according to the number of sulfate molecules bound in the channels of the mineral structure, and therefore, the Fe/S molar ratio of schwertmannite could range from 4.6 to 8.[10] Thus, the Fe/S ratios determined for pilot plant samples (6.1 to 6.6) and the sample S6 from the EHS6 culture (5.1) fit well in the range for typical schwertmannite Fe/S ratios (Table 2).

Bacteria-Mineral Associations. Electron micrographs of the pilot plant samples, as well as those of samples from shake-flask cultures of strain EHS6, did not reveal visible encrustation of bacterial cells by schwertmannite minerals. Bacteria were usually

observed in some distance to the minerals, and their cell wall remained free of iron mineral deposits.

Different observations have been made by several studies on neutrophilic iron-oxidizing[4,5,8,39,40] as well as acidophilic iron-oxidizing[34] bacteria, that showed mineralized cells and demonstrated the incorporation of organic material into mineral aggregates. The authors concluded that bacteria were not just providing ferric iron but also act as sorption surface for dissolved species and, therefore, as a nucleation site that can locally affect the physical and chemical nature of minerals.[41] Observations of encrustation-free cells, as found in the present study, were also made in studies with phototrophic iron-oxidizers at neutral pH.[40] In contrast to studies with neutrophilic strains, the pH of the surrounding medium in cultures of acidophiles is low enough to prevent initial Fe-mineral precipitation on the cells. The low pH environment allows the ferric iron ions to diffuse away from the cell, because of their higher solubility at low pH values.[8]

In general, the surface of gram-negative bacteria is negatively charged due to the carboxylate groups,[42] which would be a preferred binding site for positively charged Fe^{3+} and schwertmannite particles, respectively. However, to survive under low pH conditions, acidophilic bacteria have to maintain their neutral cytoplasmatic pH, e.g., by reversing their membrane potential while accumulating potassium ions.[43] In comparison to neutrophiles, acidophiles have a positive membrane potential and a large ΔpH across their plasma membrane, which causes a positive cell surface charge.[44] Iron minerals with a positive surface charge, like schwertmannite, would therefore be rejected from the cell surface by charge repulsion, which could be another reason for the nonencrustation of cells of the acidophilic strain EHS6 and cells observed in pilot plant samples. This underlines the influence of the positive charge repulsion of the cell surface of acidophiles on encrustation by minerals.

Since the species *Fv. myxofaciens* is known to form massive amounts of EPS in liquid media,[25] another possible explanation for the nonencrustation of bacterial could be that EPS capture ferric iron ions and act as a nucleation site. However, no encrustation of the exopolymeric structures could be detected in the present study with strain EHS6. This may be due to the presence of primarily neutral EPS molecules in biofilms of strain EHS6. While acidic EPS were detected in planktonic samples of EHS6 by cationic colloidal ThO_2 staining (Figure 1b), the EPS of biofilm samples remained unstained.

The nitrogen and TOC content in the minerals indicate a low organic content in the samples which is comparable to literature data.[46] In contrast, studies on the mineralization of EPS at a more neutral pH reported the association of organic material with the formed iron oxyhydroxides[16,39,47] and, additionally, the encrustation of EPS material of *Acidithiobacillus ferrooxidans* during leaching of pyrite has been reported.[2] Concerning the commercial use of the pilot plant, the lack of encrustation of the bacterial cells is positive for the possibility of an ongoing metabolism even in massive mineral layers, as the bacteria can still get access to ferrous iron and other nutrients to maintain ferrous iron oxidation as the key process in the pilot plant. To confirm this presumption, a depth profile of the mineral layer from the carrier material in the pilot plant should be investigated for microbial activity using fluorescent microscopy or molecular biological methods targeting active cells. Furthermore, this presumption would negate the contention that iron-oxidation in the pilot plant, as the limiting step in schwertmannite formation in the plant, could be hindered by the encrustation of bacterial cells.[48]

■ ASSOCIATED CONTENT

Ⓢ Supporting Information. Detailed description of mine water analysis, mineral analysis, EF-TEM and ESI-settings, bacterial culture growth, results of X-ray diffraction, additional electron microscopy pictures, and EELS measurements. This material is available free of charge via the Internet at http://pubs.acs.org.

■ AUTHOR INFORMATION

Corresponding Author

*Tel.: +44-1248-382832. Fax: +44 1248 370731. E-mail: s.hedrich@bangor.ac.uk.

Present Addresses

[⊥]School of Biological Sciences, College of Natural Sciences, Bangor University, Deiniol Road, Bangor LL57 2UW, U.K.

[¶]Department of Proteomics, Helmholtz Centre for Environmental Research−UFZ, Permoser Str. 15, D-04318 Leipzig, Germany.

■ ACKNOWLEDGMENT

S.H. was funded by a PhD scholarship of the German Federal Environmental Foundation (DBU) and is thankful to D.B. Johnson and K.B. Hallberg (Bangor University) for teaching the overlay plate technique and helpful comments for isolating *Fv. myxofaciens*. We are grateful to E. Janneck, F. Glombitza, and all other co-workers of G.EOS Freiberg GmbH for the operation of the pilot plant, for providing mineral samples and chemical data on the water, and for their helpful information and discussions. The skillful sample preparation for EF-TEM analysis by I. Kristen (VAM, HZI Braunschweig) is gratefully acknowledged. We thank U. Erler and the Eurofins-aua GmbH Freiberg team for the analysis of TOC and nitrogen in the mineral samples and A. Plessow and his co-workers at the Interdisciplinary Environmental Research Center, TUBAF for XRF and ICP-OES analysis of mineral samples.

■ REFERENCES

(1) Blake, R.; Johnson, D. B. Phylogenetic and biochemical diversity among acidophilic bacteria that respire on iron. In *Environmental Microbe-Metal Interactions*; Lovley, D. R., Ed.; ASM Press: Washington, D.C., 2000; pp 53−78.

(2) Frankel, R. B.; Bazylinski, D. A. Biologically induced mineralization by bacteria. *Rev. Mineral. Geochem.* **2003**, *54*, 95–114.

(3) Hallbeck, L.; Pedersen, K. Benefits associated with the stalk of *Gallionella ferruginea*, evaluated by comparison of a stalk-forming and a non-stalk-forming strain and biofilm studies in situ. *Microb. Ecol.* **1995**, *30*, 257–268.

(4) Hallberg, R.; Ferris, F. G. Biomineralization by *Gallionella*. *Geomicrobiol. J.* **2004**, *21*, 325–330.

(5) Chan, C. S.; de Stasio, G.; Welch, S. A.; Girasole, M.; Frazer, B. H.; Neterova, M. V.; Fakra, S.; Banfield, J. F. Microbial polysaccharides template assembly of nanocrystal fibers. *Science* **2004**, *303*, 1656–1658.

(6) Banfield, J. F.; Welch, S. A.; Zhang, H.; Thomson, E. T.; Penn, R. L. Aggregation-based crystal growth and microstructure development in natural iron oxyhydroxide biomineralization products. *Science* **2000**, *289* (5480), 751–754.

(7) Ferris, F. G.; Schultze, S.; Witten, T. C.; Fyfe, W. S.; Beveridge, T. J. Metal interactions with microbial biofilms in acidic and neutral pH environments. *Appl. Environ. Microbiol.* **1989**, *55* (5), 1249–1257.

(8) Schädler, S.; Burkhardt, C.; Hegler, F.; Straub, K. L.; Miot, J.; Benzerara, K.; Kappler, A. Formation of cell-iron-mineral aggregates by phototrophic and nitrate-reducing anaerobic Fe(II)-oxidizing bacteria. *Geomicrobiol. J.* **2009**, *26*, 93–103.

(9) Kappler, A.; Newman, D. K. Formation of Fe(III)-minerals by Fe(II)-oxidizing photoautotrophic bacteria. *Geochim. Cosmochim. Acta* **2004**, *68* (6), 1217–1226.

(10) Bigham, J. M.; Schwertmann, U.; Carlson, L.; Murad, E. A poorly crystallized oxyhydroxysulfate of iron formed by bacterial oxidation of Fe(II) in acidic mine waters. *Geochim. Cosmochim. Acta* **1990**, *54*, 2743–2758.

(11) Kawano, M.; Tomita, K. Geochemical modeling of bacterially induced mineralization of schwertmannite and jarosite in sulfuric acid spring water. *Am. Mineral.* **2001**, *86*, 1156–1165.

(12) Liao, Y.; Zhou, L.; Liang, J.; Xiong, H. Biosynthesis of schwertmannite by *Acidithiobacillus ferrooxidans* cell suspensions under different pH conditions. *Mater. Sci. Eng., A* **2009**, *29* (1), 211–215.

(13) Schwertmann, U.; Bigham, J. N.; Murad, E. The first occurence of schwertmannite in a natural stream environment. *Eur. J. Mineral.* **1995**, *7*, 547–552.

(14) Ferris, F. G.; Hallbeck, L.; Kennedy, C. B.; Pedersen, K. Geochemistry of acidic Rio Tinto headwaters and role of bacteria in solid phase metal partitioning. *Chem. Geol.* **2004**, *212*, 291–300.

(15) Fortin, D.; Davis, B.; Southam, G.; Beveridge, T. J. Biogeochemical phenomena induced by bacteria within sulfidic mine tailings. *J. Ind. Microbiol.* **1995**, *14*, 178–185.

(16) Benzerara, K.; Morin, G.; Yoon, T. H.; Miot, J.; Tyliszczak, T.; Casiot, C.; Bruneel, O.; Farges, F.; Brown, G. E., Jr. Nanoscale study of As biomineralization in an acid mine drainage system. *Geochim. Cosmochim. Acta* **2008**, *72*, 3949–3963.

(17) Lei, J.; Huaiyang, Z.; Xiaotong, P.; Zhonghao, D. The use of microscopy techniques to analyze microbial biofilm of the bio-oxidized chalcopyrite surface. *Min. Eng.* **2009**, *22* (1), 37–42.

(18) Eneroth, E.; Bender-Koch, C. Fe-hydroxysulphates from bacterial Fe^{2+} oxidation. *Hyperfine Interact.* **2004**, *156/157*, 423–429.

(19) Heinzel, E.; Hedrich, S.; Janneck, E.; Glombitza, F.; Seifert, J.; Schlömann, M. Bacterial diversity in a mine water treatment plant. *Appl. Environ. Microbiol.* **2009**, *75* (3), 858–861.

(20) Hallberg, K. B. New perspectives in acid mine drainage microbiology. *Hydrometallurgy* **2010**, *104*, 448–453.

(21) Glombitza, F.; Janneck, E.; Arnold, I.; Rolland, W.; Uhlmann, W. Eisenhydroxysulfate aus der Bergbauwasserbehandlung als Rohstoff. In *Consulting-Erfahrungen und Kontakte für Neuanfänge - Untertägiger Bergbau und Industrieminerale in Deutschland, GDMB Gesellschaft für*; Bergbau, R.-u. U. e. V., Ed. GDMB Medienverlag: Clausthal-Zellerfeld, Germany, 2007; Vol. 10.

(22) Heinzel, E.; Janneck, E.; Glombitza, F.; Schlömann, M.; Seifert, J. Population dynamics of iron-oxidizing communities in pilot plants for the treatment of acid mine waters. *Environ. Sci. Technol.* **2009**, *43* (16), 6138–6144.

(23) Johnson, D. B.; Hallberg, K. B. Techniques for detection and identifying acidophilic mineral-oxidising microorganisms. In *Biomining*; Rawlings, D. E., Johnson, D. B., Eds.; Springer-Verlag: Berlin, Heidelberg, 2007; pp 237−262.

(24) Hedrich, S.; Heinzel, E.; Seifert, J.; Schlömann, M. Isolation of novel iron-oxidizing bacteria from an acid mine water treatment plant. *Adv. Mat. Res.* **2009**, *71−73*, 125–128 (Biohydrometallurgy).

(25) Rowe, O. F.; Johnson, D. B. Comparison of ferric iron generation by different species of acidophilic bacteria immobilized in packed-bed reactors. *Syst. Appl. Microbiol.* **2008**, *31*, 68–77.

(26) Lovley, D. R.; Phillips, E. J. Rapid assay for microbially reducible ferric iron in aquatic sediments. *Appl. Environ. Microbiol.* **1987**, *53* (7), 1536–1540.

(27) Lünsdorf, H.; Strömpl, C.; Osborn, A. M.; Bennasar, A.; Moore, E. R.; Abraham, W. R.; Timmis, K. N. Approach to analyze interactions of microorganisms, hydrophobic substrates, and soil colloids leading to formation of composite biofilms, and to study initial events in microbiogeological processes. *Method Enzymol.* **2001**, *336*, 317–331.

(28) Lünsdorf, H.; Kristen, I.; Barth, E. Cationic hydrous thorium dioxide colloids−a useful tool for staining negatively charged surface matrices of bacteria for use in energy-filtered transmission electron microscopy. *BMC Microbiol.* **2006**, *6*, 59.

(29) Bigham, J. M.; Carlson, L.; Murad, E. Schwertmannite, a new iron oxyhydroxysulphate from Pyhäsalmi, Finland, and other localities. *Mineral. Mag.* **1994**, *58*, 641–648.

(30) Thiéry, J. Mise en évidence des polysaccharides sur coupes fines en microscopie électronique. *J. Microscop.* **1967**, *9*, 87–94.

(31) Moore, K. T. X-ray and electron microscopy of actinide materials. *Micron* **2010**, *41*, 336–358.

(32) Brydson, R.; Koehler, A. In *Electron Energy Loss Spectroscopy*; Life Sciences, Eds.; Microscopic Handbooks Vol. 48; BIOS Scientific Publishers Ltd (in association with the Royal Microscopical Society): Oxford, UK, 2006.

(33) Wang, H.; Bigham, J. M.; Tuovinen, O. H. Formation of schwertmannite and its transformation to jarosite in the presence of acidophilic iron-oxidizing microorganism. *Mater. Sci. Eng., C* **2006**, *26*, 588–592.

(34) Ferris, F. G.; Tazaki, K.; Fyfe, W. S. Iron oxides in acid mine drainage environments and their association with bacteria. *Chem. Geol.* **1989**, *74*, 321–330.

(35) Regenspurg, S.; Brand, A.; Peiffer, S. Formation and stability of schwertmannite in acidic mining lakes. *Geochim. Cosmochim. Acta* **2004**, *68*, 1185–1197.

(36) Barham, R. J. Schwertmannite: A unique mineral, contains a replaceable ligand, transforms to jarosites, hematites, and/or basic iron sulfate. *J. Mat. Res.* **1997**, *12* (10), 2751–2758.

(37) Gramp, J. P.; Jones, F. S.; Bigham, J. M.; Tuovinen, O. H. Monovalent cation concentrations determine the types of Fe(III) hydroxysulfate precipitates formed in bioleach solutions. *Hydrometallurgy* **2008**, *94*, 29–33.

(38) Twidwell, L. G.; Gammons, C. H.; Young, C. A.; Berg, R. B. Summary of deepwater sediment/pore water characterization for the metal-laden Berkeley Pit Lake in Butte, Montana. *Mine Water Environ.* **2006**, *25* (2), 86–92.

(39) Chan, C. S.; Fakra, S. C.; Edwards, D. C.; Emerson, D.; Banfield, J. F. Iron oxyhydroxide mineralization on microbial extracellular polysaccharides. *Geochim. Cosmochim. Acta* **2009**, *73*, 3807–3818.

(40) Miot, J.; Benzerara, K.; Obst, M.; Kappler, A.; Hegler, F.; Schädler, S.; Bouchez, C.; Guyot, F.; Morin, G. Extracellular iron biomineralization by photoautotrophic iron-oxidizing bacteria. *Appl. Environ. Microbiol.* **2009**, *75* (17), 5586–5591.

(41) Fortin, D.; Ferris, F. G. Precipitation of iron, silica, and sulfate on bacterial cell surfaces. *Geomicrobiol. J.* **1998**, *15*, 309–324.

(42) Beveridge, T. J. Role of cellular design in bacterial metal accumulation and mineralization. *Annu. Rev. Microbiol.* **1989**, *43*, 147–171.

(43) Baker-Austin, C.; Dopson, M. Life in acid: pH homeostasis in acidophiles. *Trends Microbiol.* **2007**, *15* (4), 165–171.

(44) Ingledew, W.; Norris, P. Acidophilic bacteria: adaptations and applications. In *Molecular Biology and Biotechnology of Extremophiles*; Hebert, R.; Sharp, R., Eds.; Blackie: Glasgow, 1992; pp 115−142.

(45) Dupraz, C.; Reid, P. R.; Braissant, O.; Decho, A. W.; Norman, R. S.; Visscher, P. T. Processes of carbonate precipitation in modern microbial mats. *Earth-Sci. Rev.* **2009**, *96*, 141–162.

(46) Kumpulainen, S.; Raisanen, M.-L.; von der Kammer, F.; Hofmann, T. Aging of synthetic and natural schwertmannite at pH 2−8. *Clays Clay Miner.* **2008**, *43*, 437–448.

(47) Miot, J.; Benzerara, K.; Morin, G.; Kappler, A.; Bernard, S.; Obst, M.; Ferard, C.; Skouri-Panet, F.; Guigner, J.-M.; Posth, N.; Galvez, M.; Brown, G. E. J.; Guyot, F. Iron biomineralization by anaerobic neutrophilic iron-oxidizing bacteria. *Geochim. Cosmochim. Acta* **2009**, *73* (3), 696–711.

(48) Hegler, F.; Schmidt, C.; Schwarz, H.; Kappler, A. Does a low-pH microenvironment around phototrophic Fe(II) -oxidizing bacteria prevent cell encrustation by Fe(III) minerals? *FEMS Microbiol. Ecol.* **2010**, *74* (3), 592–600.